OXFORD

SOT | Society of Toxicology
www.toxsci.oxfordjournals.org

TOXICOLOGICAL SCIENCES, 153(1), 2016, 165–173

doi: 10.1093/toxsci/kfw116
Advance Access Publication Date: July 27, 2016
Research article

Lower Fractional Anisotropy in the Globus Pallidus of Asymptomatic Welders, a Marker for Long-Term Welding Exposure

Eun-Young Lee,* Michael R. Flynn,† Guangwei Du,* Mechelle M. Lewis,*,‡ Amy H. Herring,§ Eric Van Buren,§ Scott Van Buren,§ Lan Kong,¶ Richard B. Mailman,*,‡ and Xuemei Huang*,‡,||,|||,||||,1

*Department of Neurology, Pennsylvania State University-Milton S. Hershey Medical Center, Hershey, Pennsylvania 17033; †Department of Environmental Sciences and Engineering, University of North Carolina, Chapel Hill, North Carolina 27599; ‡Department of Pharmacology, Pennsylvania State University-Milton S. Hershey Medical Center, Hershey, Pennsylvania 17033; §Department of Biostatistics, University of North Carolina, Chapel Hill, North Carolina 27599; and, ¶Department of Public Health Sciences; ||Department of Radiology; |||Department of Neurosurgery; and ||||Department of Kinesiology, Pennsylvania State University-Milton S. Hershey Medical Center, Hershey, Pennsylvania 17033

[1]To whom correspondence should be addressed Department of Neurology, Penn State University-Milton S. Hershey Medical Center, H037, 500 University Drive, Hershey, Pennsylvania 17033-0850. Fax: 717-531-0266; E-mail: Xuemei@psu.edu.

ABSTRACT

Introduction: Welding fumes contain several metals including manganese (Mn), iron (Fe), and copper (Cu) that at high exposure may co-influence welding-related neurotoxicity. The relationship between brain accumulation of these metals and neuropathology, especially in welders with subclinical exposure levels, is unclear. This study examined the microstructural integrity of basal ganglia (BG) regions in asymptomatic welders using diffusion tensor imaging (DTI). **Methods**: Subjects with (n = 43) and without (age- and gender-matched controls; n = 31) history of welding were studied. Occupational questionnaires estimated short-term (HrsW; welding hours and E_{90}; cumulative exposure, past 90 days) and long-term (YrsW; total years welding and ELT; cumulative exposure, lifetime) exposure. Whole blood metal levels (Mn, Fe, and Cu) were obtained. Brain MRI pallidal index (PI), R1 (1/T1), and R2* (1/T2*) were measured to estimate Mn and Fe accumulation in BG [caudate, putamen, and globus pallidus (GP)]. DTI was used to assess BG microstructural differences, and related with exposure measurements. **Results**: When compared with controls, welders had significantly lower fractional anisotropy (FA) in the GP. In welders, GP FA values showed non-linear relationships to YrsW, blood Mn, and PI. GP FA decreased after a critical level of YrsW or Mn was reached, whereas it decreased with increasing PI values until plateauing at the highest PI values. GP FA, however, did not show any relationship with short-term exposure measurements (HrsW, E_{90}), blood Cu and Fe, or R^{2*} values. **Conclusion**: GP FA captured microstructural changes associated with chronic low-level Mn exposure, and may serve as a biomarker for neurotoxicity in asymptomatic welders.

Key words: welders; diffusion tensor imaging; fractional anisotropy; globus pallidus; pallidal index; manganese.

Welding, especially at high-exposure levels, has been associated with neurobehavioral disorders such as manganese-induced parkinsonism (Cersosimo and Koller, 2006; Lucchini *et al.*, 2009; Racette *et al.*, 2012; Wang *et al.*, 1989). Welding fumes, however, contain several metals including manganese (Mn), iron (Fe), and copper (Cu) that may co-influence welding-related neurotoxicity (Choi *et al.*, 2007; Flynn and Susi, 2009; Lee *et al.*, 2015). Although previous studies focused on selective Mn accumulation in basal ganglia (BG), especially the globus pallidus (GP; Lucchini *et al.*, 2000), the relationship between brain accumulation of Mn and/or other welding-related metals and neuronal pathology, especially at subclinical exposures, is unclear.

Diffusion weighted imaging (DWI; Schaefer *et al.*, 2000) and diffusion tensor imaging (DTI; Basser and Pierpaoli, 1996; Le Bihan *et al.*, 2001) are forms of MRI that can assess tissue microstructural properties by measuring diffusion, the random translational motion of water molecules (Basser and Pierpaoli, 1996). These MRI modalities have been used to investigate Mn- and/or welding-related microstructural changes, but the findings have been inconsistent. For example, in asymptomatic welders (Criswell *et al.*, 2012) or in a Mn-intoxicated patient (McKinney *et al.*, 2004), there was a reduction in the magnitude of overall diffusion [i.e., lower apparent diffusion coefficient (ADC) values of DWI] in the GP. Conversely, an increase in the overall diffusion magnitude (ie, higher mean diffusivity [MD] values of DTI) in the GP was reported after Mn overload caused by intravenous methcathinone abuse (Stepens *et al.*, 2010). No studies have demonstrated an association between the diffusion imaging findings and degree of welding exposure.

It recently has been demonstrated that DTI fractional anisotropy (FA), a diffusion anisotropy measure that traditionally has been used to measure white matter properties and the connectivity between brain gray matter regions, may capture microstructural changes in subcortical gray matter structures (Chan *et al.*, 2007; Hashimoto *et al.*, 2009; Yoshikawa *et al.*, 2004). For example, a previous study reported that schizophrenia patients had significantly lower FA values in the GP compared with controls (Hashimoto *et al.*, 2009), suggestive of microstructural changes. Several other studies reported that Parkinson's disease patients, including drug-naïve *de novo* patients (Vaillancourt *et al.*, 2009), had lower FA values in the substantia nigra (SN; Chan *et al.*, 2007; Du *et al.*, 2011).

Although Mn-induced parkinsonism is not the same as classic Parkinson's disease, the GP of the BG is morphologically very similar to the SN (Schwyn and Fox, 1974; Yelnik *et al.*, 1984). Thus, the present study 1) tested whether DTI measures (especially FA) may detect early microstructural changes in the BG of asymptomatic welders with chronic, low-level exposure and 2) explored the associations of the DTI measures with welding exposure levels.

METHODS

Study Subjects

Eighty subjects were recruited initially from unions in central Pennsylvania and surrounding communities. Welders were defined as subjects who had welded at any point in their lifetime, and controls as those without history of welding. All subjects were male, answered negatively for past Parkinson's diagnosis or other neurological disorders, and were free of any obvious neurological or movement deficits using the Unified Parkinson's Disease Rating Scale-motor scores (UPDRS-III) with a threshold score of <15 (Lee *et al.*, 2015). Written informed consent was obtained in accordance with guidelines approved by the Penn State Hershey Institutional Review Board.

Welders represented several different trades and industry groups (eg, boilermakers, pipefitters, railroad welders, and a variety of other manufacturing jobs). Controls were age- and gender-matched volunteers from various occupations but from communities in the same region. Six subjects either failed to complete the DTI acquisition (2 welders and 1 control) or had poor image co-registration (2 welders and 1 control). These were excluded from the analysis resulting in 31 controls and 43 welders (Table 1).

Exposure Assessment and Blood Analysis

Exposure first was assessed by the work history (WH; Lee *et al.*, 2015) questionnaire that collected job information over the individual's working lifetime, emphasizing welding and other jobs associated with welding exposure. Responses to the WH questionnaire enabled 2 cumulative lifetime welding estimates (YrsW = years spent welding during the subjects' life and ELT = an estimate of cumulative exposure to inhaled Mn over the individual's life; Supplementary Materials 1a) (Lee *et al.*, 2015). An additional supplementary exposure questionnaire focused on the 90-day period prior to the MRI, and ascertained the time spent welding, type of metal welded, and various types of welding performed (supplemental exposure questionnaire (SEQ); Lee *et al.*, 2015). The exposure metrics derived from the SEQ were: hours welding, brazing, or soldering (HrsW = [weeks worked] * [h/week] * [fraction of time worked related directly to welding]) and E_{90} (an estimate of the cumulative 90 day exposure to Mn; Supplementary Material 1b) in the 90 day period preceding the MRI (Lee *et al.*, 2015). Whole blood Cu, Fe, and Mn levels were measured by Inductively Coupled Plasma Mass Spectrometry in batches from samples that had been collected the morning of the MRI acquisition and then stored at -80 °C until analysis.

MR Image Acquisition and Image Processing

All images were acquired using a Siemens 3T scanner (Magnetom Trio, Erlangen, Germany) with an 8-channel head coil. First, high-resolution T1-weighted (T1W) and T2-weighted (T2W) images were acquired for anatomical segmentation and pallidal index (PI) estimation. For T1W images, MPRAGE sequences with Repetition Time (TR)/Echo Time (TE) =1540/2.3 ms, FoV/matrix = 256 × 256/256 × 256 mm, slice thickness = 1 mm, slice number = 176 (with no gap), and voxel spacing 1 × 1 × 1 mm were used. For T2W images, fast-spin-echo sequences of TR/TE = 2500/316 ms were used with the same spatial resolution as the T1W images. For R1, TR/TE = 15/1.45 ms, flip angles = 4/25, FoV/matrix = 250 × 250/160 × 160 mm, slice thickness = 1 mm, slice number = 192, and voxel spacing = 1.56 × 1.56 × 1 mm were used. For R2*, 5 TEs ranging from 8 to 40 ms with an interval of 8 ms, TR = 51 ms, flip angle = 15°, FoV/matrix = 230 × 230/256 × 256 mm, slice thickness = 1.6 mm, and slice number = 88 were used. For DTI, TR/TE = 8300/82 ms, 42 diffusion gradient directions with b = 1000 s/mm^2, and 7 b = 0 s/mm^2 scans, FoV/matrix = 256 × 256/128 × 128 mm, slice thickness = 2 mm, and slice number = 65 were used.

Defining Brain Regions of Interest

Bilateral BG structures (GP, putamen [PUT], and caudate nucleus [CN]) were selected as regions of interest (ROI; Chang *et al.*, 2009; Criswell *et al.*, 2012; Dorman *et al.*, 2006). ROIs were defined for each subject using automatic segmentation software (AutoSeg; Gouttard *et al.*, 2007; Joshi *et al.*, 2004) and then eroded by 1 voxel using a morphological operation in order to ensure the segmented ROI was within the anatomical ROI (Lee *et al.*, 2015). The segmentation quality then was confirmed visually by a reviewer blinded to the group assignment.

TABLE 1. Summary Statistics for Demographics (I), Exposure Metrics and Blood Metals (II), and MRI Measures (III) in Welders and Controls.

	Welders (n = 43) Mean ± SD	Controls (n = 31) Mean ± SD	Raw P-values
I. Demographics			
Age (years)	48.6 ± 10.8	43.6 ± 11.4	.078
Education (years)	12.8 ± 1.6	16.3 ± 2.3	<.001
ALT (IU/L)	39.2 ± 17.2	38.1 ± 16.5	.511
BMI (kg/m^2)	29.3 ± 4.9	26.1 ± 3.3	.003
Hemoglobin	15.2 ± 1.0	14.9 ± 0.8	.157
UPDRS-III	2.0 ± 2.5	1.5 ± 2.1	.226
II. Exposure metrics and whole blood metal levels			
HrsW (hours)	244 ± 199	0 ± 0	<.001
E_{90} mg-d/m^3	2.3 ± 2.0	0.003 ± 0	<.001
YrsW (years)	26.1 ± 10.8	0.0 ± 0	<.001
ELT mg-years/m^3	1.16 ± 0.78	0.001 ± 0.0003	<.001
Whole Cu (ng/ml)	890 ± 126	745 ± 133	<.001
Whole Mn (ng/ml)	11.0 ± 3.2	8.8 ± 2.5	.003
Whole Fe (μg/ml)	555 ± 53	499 ± 75	<.001
III. MRI PI, R1, and R2 values*			
PI	109.5 ± 2.44	109.0 ± 1.85	.463
R1 CN	0.68 ± 0.07	0.66 ± 0.05	.396
R1 PUT	0.71 ± 0.05	0.70 ± 0.05	.584
R1 GP	0.89 ± 0.06	0.87 ± 0.06	.727
R2* CN	22.9 ± 2.24	21.8 ± 1.73	.007*
R2* PUT	27.1 ± 3.17	26.0 ± 3.00	.032
R2* GP	36.6 ± 4.6	36.3 ± 5.28	.343

P-values for R1 and R2* measures indicate pairwise comparisons and *indicates comparisons that remained significant at $P < .05$ after correction for multiple group comparisons using the Stepdown Bonferroni method.

Estimations of Brain MRI Measurements

DTI values. DTI quality control and tensor reconstruction were performed using DTIPrep (University of North Carolina, Chapel Hill, North Carolina) that first checks diffusion images for appropriate quality by calculating the inter-slice and inter-image intra-class correlation, and then corrects for the distortions induced by eddy currents and head motion (Liu *et al.*, 2010). DTI maps then were estimated via weighted least squares (Salvador *et al.*, 2005). The segmented ROIs on T1W images were co-registered first onto T2W images using FSL Flirt. DTI maps then were co-registered onto T2W images using ANTS, and the transformation matrix was inversely applied to bring ROIs on the T2W images to the DTI maps. Mean DTI values in the ROIs of each subject were calculated using trimmed means (5–95% percentile) to reduce the influence of possible segmentation error and imaging noise (Supplementary Figure S1).

Four DTI values (FA, AD [axial diffusivity], RD [radial diffusivity], and MD) were calculated out of 3 diffusivity eigenvalues ($\lambda 1$, $\lambda 2$, $\lambda 3$) (Le Bihan *et al.*, 2001). FA is a weighted average of pairwise differences of the 3 eigenvalues and may represent the degree of diffusion anisotropy.

$$FA = \sqrt{\frac{1}{2}}\frac{\sqrt{(\lambda_1-\lambda_2)^2+(\lambda_2-\lambda_3)^2+(\lambda_3-\lambda_1)^2}}{\sqrt{(\lambda_1^2+\lambda_2^2+\lambda_3^2)}}$$

AD and RD gauge the orientation of the diffusion anisotropy: AD is the largest main eigenvalue ($\lambda 1$) along the axis of maximum diffusion, whereas RD is an average of the remaining 2 eigenvalues. DTI MD is an average of the 3 eigenvalues, providing the overall diffusion magnitude that is comparable to the traditional ADC of DWI with more than one diffusion direction (Le Bihan *et al.*, 2001). For DTI, images are acquired by applying at least 6 gradient directions that enable measurement of water movement in 3 dimensions based on the diffusion tensor matrix (Backens, 2015; Basser, 1995; Schaefer *et al.*, 2000). For DWI, images typically are obtained with gradients applied in one direction (Stejskal and Tanner, 1965) and ADC is an estimate of the magnitude of diffusion for the one specific gradient direction. Image acquisition with multiple gradient directions leads to creation of multiple ADC values and the mean of these multiple ADC values is mathematically comparable to DTI MD.

R1 values. Longitudinal relaxation rate (R1; 1/T1) is an estimate of Mn brain accumulation (Lee *et al.*, 2015) because Mn has paramagnetic characteristics and can shorten the MRI longitudinal relaxation time (T1) and increase T1-weighted intensity (T1WI). To estimate R1 values, whole brain T1 time images were generated by the scanner using a published method (Venkatesan *et al.*, 1998). ROIs were co-registered onto the T1 maps using an affine registration implemented in 3D Slicer (www.slicer.org; Rueckert *et al.*, 1999). The R1 values of each ROI were calculated as 1/T1 in each voxel and averaged over the entire ROI using a trimmed mean (5–95% percentile) (Lee *et al.*, 2015).

Pallidal index. To calculate the PI (an estimate of Mn accumulation in the GP), T1W images were skull stripped and then a bias field correction was used to correct within-subject intensity variations caused by imperfect magnetic fields. Next, histogram-based intensity standardization was used to reduce magnet field inhomogeneity between subjects (Ge *et al.*, 2000; Nyúl *et al.*, 2000; Sen *et al.*, 2011). Subsequently, the GP and frontal white matter (FWM) ROIs were mapped onto the intensity-corrected T1W images (co-registration). The mean intensities of the individual ROI for each subject were calculated using a trimmed mean (5–95% percentile) to reduce possible segmentation error and imaging noise. The PI was derived from the ratio of GP T1W intensity to FWM intensity [PI = (GP/FWM) × 100] (Krieger *et al.*, 1995).

*R2*values*. The apparent transverse relaxation rate (T2*; Haacke *et al.*, 2005) is an estimate for Fe brain because Fe has paramagnetic characteristics and shortens the apparent transverse relaxation time (T2*; Haacke *et al.*, 2005). To calculate R2* values, the magnitude images of multigradient-echo images were used to generate R2* maps by using a voxel-wise linear least-squares fit to a monoexponential function with free baseline using in-house MATLAB (The MathWorks, Inc., Natick, MA) tools. The automatically segmented ROIs on the T1W images first were co-registered onto T2W images, and then the ROIs on T2W image space were co-registered again onto the R2* maps using an affine registration implemented in 3D Slicer (www.slicer.org; Rueckert *et al.*, 1999). R2* values in each ROI were calculated as 1/T2* in each voxel and averaged over the entire ROI (Du *et al.*, 2011; Lee *et al.*, 2016).

Statistical Analysis

Group comparisons were conducted using 1-way analysis of variance (ANOVA). For MRI DTI, R1, and R2* measures, repeated measures ANOVAs based on mixed models were conducted by treating group (controls versus welders) as a between-subjects factor and ROI as a within-subjects factor. The mixed model analyses were adjusted for age, body mass index (BMI), respirator use, and the group × BMI interaction term. For the R2* or R1

measures, the analyses were additionally adjusted by R1 or R2* values, and whole blood metal levels of Mn and Cu (for R2* analysis) or Fe and Cu (for R1 analysis) as covariates. Because the primary interest was to examine group differences for each ROI, post hoc pairwise group comparisons for each ROI were conducted using t-tests even if the group × ROI interaction failed to reach significance. Since there were 3 ROIs to be compared, the pairwise comparisons were corrected for multiple comparisons using the Stepdown Bonferroni method (Holm, 1979) to control the familywise error rate (*FWER*) at $P = .05$. We reported significant results with *FWER*-corrected *p* values but marginally significant effects also were reported when they were judged likely to be of interest to the readers.

To examine dose-response associations in welders, DTI measures that showed significant pairwise group differences were plotted against estimated welding exposure measures (exposure metrics; blood metal levels; MRI PI, R1, and R2* in the corresponding ROI) using Lowess plots (Supplementary Figures S2–S4). The possible dose-response relationships then were first tested using Pearson partial correlation analyses with adjustment for age. For the associations between DTI measures and blood metal levels of interest, Pearson partial correlations additionally were adjusted for the other blood levels. In order to further explore possible polynomial relationships between the DTI measures and the estimated welding exposure measures within welders, regression models were used after adjusting for age. Statistical significance was defined by $\alpha = 0.05$. SAS 9.3 was used for all statistical analyses.

RESULTS

Group Comparisons

Demographics

There were no significant differences in age, hemoglobin, liver function (ALT; alanine aminotransferase), or UPDRS-III scores between controls and welders (Table 1). Controls had more education years than welders ($P < .001$). Welders had a higher BMI than controls ($P = .003$).

Welding Exposure-Related Measurements

Exposure Metrics and Whole Blood Metal Levels

Welders had greater HrsW (244 ± 199 h), E_{90} (2.3 ± 2.0 mg-d/m^3 for welders and 0.003 ± 0 mg-d/m^3 for controls), YrsW (26.1 ± 10.8 years), and ELT (1.16 ± 0.78 mg-years/m^3 for welders and 0.001 ± 0.0003 mg-years/m^3 for controls) than controls (*Ps* < .001). Welders also had greater whole blood Cu (890 ± 126 ng/ml for welders and 745 ± 133 ng/ml for controls), Fe (555 ± 53 μg/ml for welders and 499 ± 75 μg/ml for controls), and Mn (11.0 ± 3.2 ng/ml for welders and 8.8 ± 2.5 ng/ml for controls) metal levels than controls (*Ps* < .003).

MRI PI, R1, and R2*Measures in the BG

For the PI, there was no group difference ($P = .46$). For R1, there were significant main effects of ROI (F [2,60] = 439.62, $P < .001$) but no significant effect of group (F[1,60] = 0.23, $P = 0.64$], group × ROI interaction (F [2,60] =0.43, $P = 0.65$), or group × BMI interaction (F[1,60] = 0.11 $P = .73$). Pairwise group comparisons for each ROI revealed no differences in any ROIs (*Ps* > 0.72).

For R2*, there were significant main effects of ROI (F[2,60] = 122.89, $P < .001$) but no significant effects of group (F [1,60] = 3.01, $P = 0.088$), group × ROI interaction (F(2,60) = 0.13, $P = .88$), or group × BMI interaction (F[1,60] = 1.55 $P = 0.22$]. Pairwise group comparisons for each ROI revealed higher R2* in the CN of welders compared with controls ($t = 2.78$, $P = .022$).

DTI Microstructural Changes in the BG

For FA, there were significant main effects of ROI (F [2,66] = 1500, $P < .001$) and group × ROI interactions (F [2,66] = 7.62, $P = .001$), but no main effect of group (F (1,66)=0.73, p = 0.40] or group × BMI interaction (F[1,66] = 1.36 $P = .25$). Pairwise group comparisons for each ROI revealed that GP FA values were significantly lower in welders compared with controls with adjustments of age, BMI, group × BMI, and respirator use, which remained significant after *FWER*-correction ($t = -3.08$, $P = .009$; Figure 1a). The significantly lower GP FA value persisted with additional adjustments of R2* and blood Cu and Fe levels ($t = -3.47$, $P = .003$). FA values were not significantly different in CN and PUT regions.

For MD, RD, and AD, there were significant main effects of ROI (*Fs* > 22.76, *Ps* < 0.001) but no significant effect of group (*Fs* < 2.13, *Ps* > 0.90), group × BMI interaction (*Fs* < 2.36, *Ps* > 0.13), or group × ROI interaction (*Fs* < 2.35, *Ps* > 0.67) except for a significant group × ROI interaction for RD [F(2,66) = 4.43, $P = 0.016$). None of the pairwise comparisons for MD, RD, or AD in any ROI showed significance after *FWER*-correction (*Ps* > 0.094, Figure 1b–d).

GP FA Associations With Welding-Related Exposure Measurements for Welders

Pearson Partial Correlation Analyses

Exposure metrics and blood metal levels. There were no significant correlations between GP FA values and exposure metrics and blood metal levels for welders (*Ps* > 0.19).

MRI PI, R1, and R2 values*. Within welders, GP FA values were negatively and linearly correlated with the PI ($R = -0.38$, $P = .013$) but not with R1 or R2* values (*Ps* > 0.23).

Assessments of Polynomial Relationships

Exposure metrics. For welders, there were no significant polynomial relationships between GP FA values and short-term exposure metrics (HrsW and E_{90}, *Ps* > 0.30; Supplementary Figure S2). GP FA values, however, showed a second-order polynomial relationship with YrsW ($\beta = -.0002$, $R^2 = 0.13$, $P = 0.028$; Figure 2a), indicating that GP FA values did not decrease until the YrsW exceeded approximately 30 YrsW (n = 32). ELT, an estimate of long-term cumulative exposure, also showed a similar relationship pattern with GP FA, but this failed to be significant ($P = .30$; Figure 2b).

Blood metals. For welders, GP FA values showed a significant second-order polynomial relationship with blood Mn levels ($\beta = -0.0008$, $R^2 = 0.11$, $P = 0.036$; Figure 2c), indicating that GP FA values started to decrease after a blood Mn level of about 13 ng/ml (n = 10). The significant non-linear relationship persisted after controlling for blood Cu and Fe levels ($P = 0.013$). There were, however, no polynomial relationships between GP FA values and blood Fe and Cu levels (*Ps* > 0.34; Supplementary Figure 3).

MRI PI, R1, and R2 values*. GP FA values in welders had a significant third-order polynomial relationship with age-adjusted PI ($\beta = 0.0002$, $R^2 = 0.30$, $P = .009$). It appeared that GP FA values decreased with increasing PI followed by a steeper decrease and

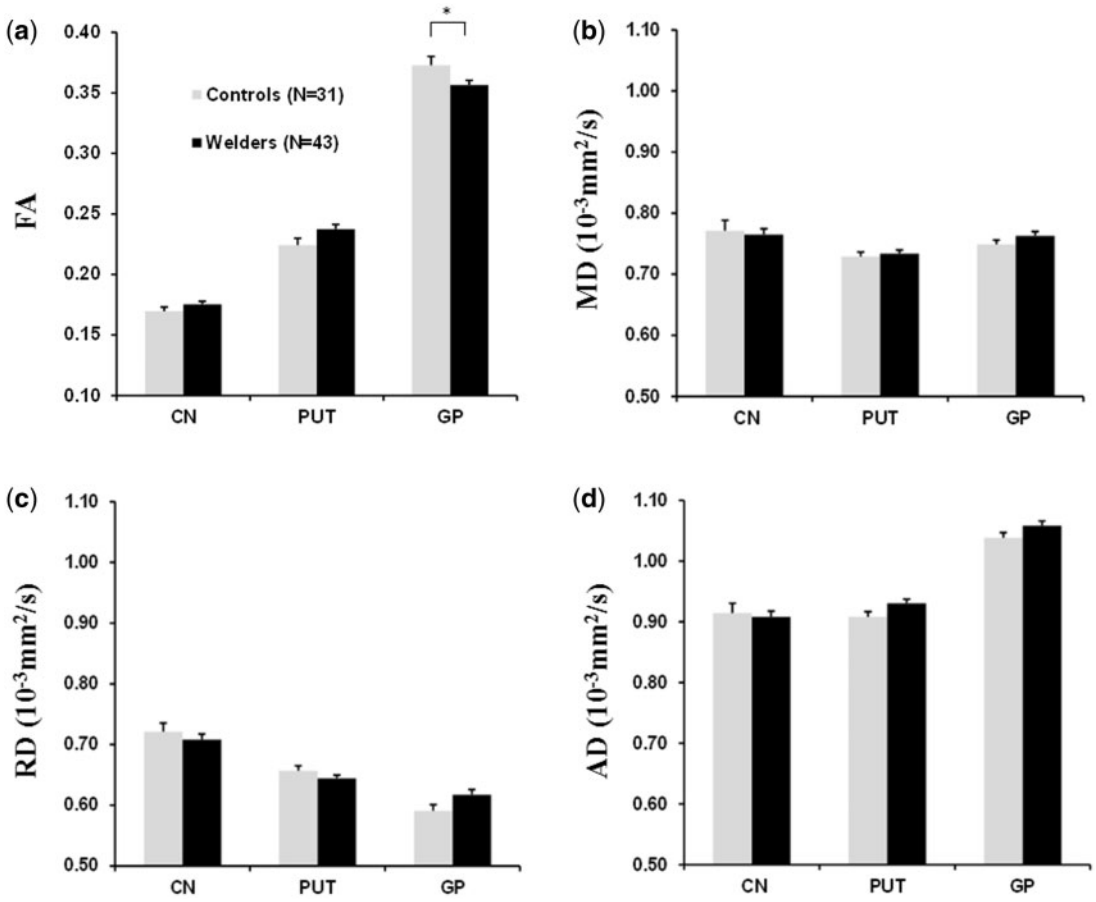

FIG. 1. MRI DTI in basal ganglia ROIs (CN, PUT, GP). **a,** FA; **b,** MD; **c,** RD; and **d,** AD (axial diffusivity) for welders and controls. Values are raw means ± SEM. *indicates significance ($P < .05$) after correction for multiple group comparisons using the using the Stepdown Bonferroni method.

then plateaued at the highest PI levels (Figure 2d and Supplementary Figure S4), whereas a second-order polynomial relationship failed to reach significance ($P = .34$). R1, another estimate of Mn brain accumulation, also showed a similar relationship pattern with GP FA but this failed to be significant ($P = .094$; Figure 2e). Conversely, GP FA values did not show any polynomial relationship with R2* values (Ps > 0.23; Supplementary Figure S4).

Post Hoc Stepwise Regression Analysis

Since GP FA values showed significant polynomial relationships with YrsW, blood Mn levels, and the PI in welders, a post hoc stepwise regression analysis was conducted collapsed across controls and welders using these variables (age-adjusted YrsW, $YrsW^2$, blood Mn, blood Mn^2, PI, PI^2, and PI^3) as predictors. The analysis demonstrated that the age-adjusted YrsW ($\beta = 0.0008$, $P = .006$) and PI ($\beta = -0.0043$, $P = .030$) were significant predictors ($R^2 = 0.171$) of GP FA values.

DISCUSSION

There have been significant efforts to seek surrogate biomarkers of Mn and/or welding-related neurotoxicity. In an asymptomatic welder cohort, the current study demonstrated that GP FA, but not MD, values were significantly lower in welders compared with controls. Moreover, in welders, GP FA values showed non-linear relationships to YrsW, blood Mn, and PI. GP FA values decreased after a critical level of YrsW or blood Mn was reached, whereas they decreased with increasing PI values and then reached a plateau at the highest PI values. Conversely, GP FA values did not show any relationship with short-term exposure metrics (HrsW and E_{90}), blood Cu and Fe levels, and R2* values. Collectively, our data suggest that lower GP FA values may capture microstructural changes associated with long-term Mn-exposure. Thus, FA may serve as a useful early marker for microstructural changes to gauge Mn neurotoxicity in asymptomatic welders and possibly other neurotoxicant-exposed populations.

FA Is Lower in the GP

There has been one report of greater (7%) MD, an overall diffusion magnitude measure, in the GP of Mn-overloaded methcathinone abusers (Stepens *et al.*, 2010). Conversely, other studies have reported lower GP ADC values for asymptomatic welders (Criswell *et al.*, 2012) or for a subject with Mn toxicity (McKinney *et al.*, 2004). We found a non-significant MD increase (1.9%) in our welders. Factors that might reconcile these differences include the effects of methcathinone abuse (Stepens *et al.*, 2010), as well as the fact that our welders have chronic but relatively low-level welding exposure: Our welders averaged 244 ± 199 welding hours (HrsW) in the past 90-days,

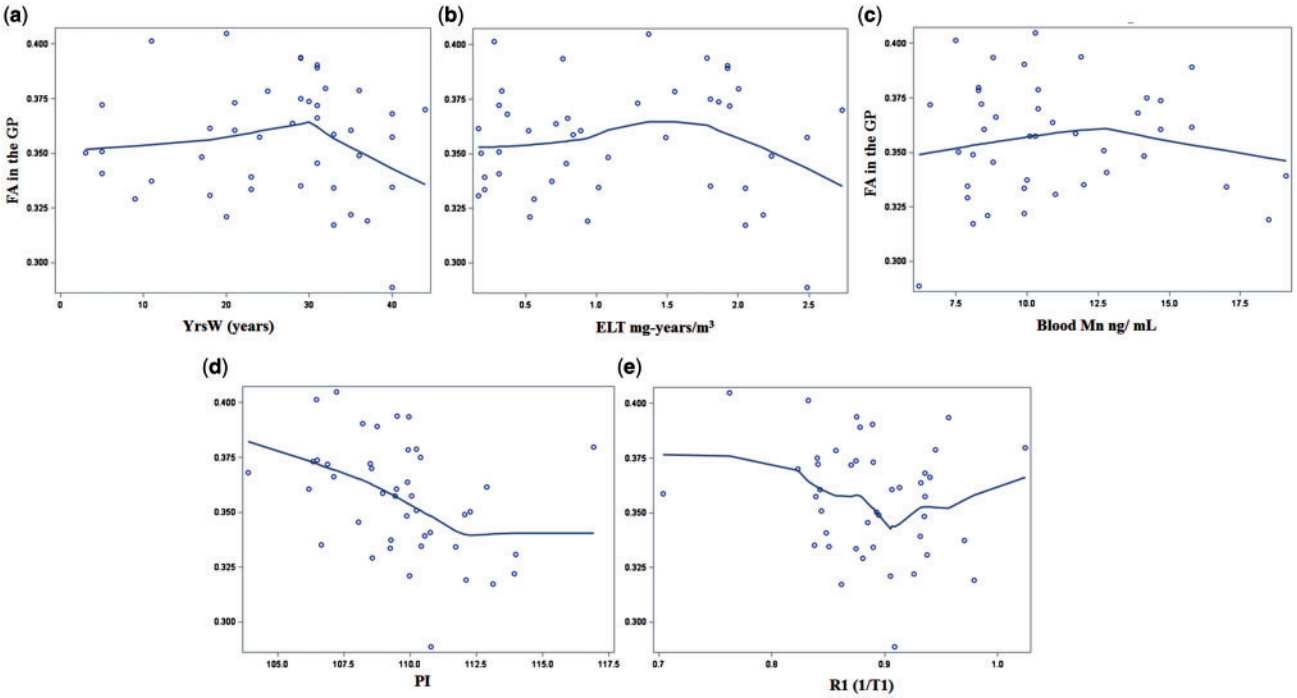

FIG. 2. LOWESS plots depicting relationships of FA in the GP with exposure measurements: **a,** YrsW; **b,** ELT; **c,** blood Mn level; **d,** PI; and **e,** R1(1/T1) for welders.

approximately equivalent to spending nearly half of their worktime welding (Lee *et al.*, 2015), with estimated cumulative exposure (E_{90}) of 2.32 ± 2.0 mg-d/m^3. They also had an average of 26.1 ± 10.8 lifetime welding years (YrsW), confirming the characteristics of chronic but low-level welding exposure, different from most previous studies that focused on high-level welding exposure (Choi *et al.*, 2007; Criswell *et al.*, 2012).

Our welders, however, displayed significantly decreased (4.4%) FA values in the GP. Although lower FA values in the GP previously were reported in schizophrenia patients (Hashimoto *et al.*, 2009), suggestive of microstructural changes in this region, FA in the GP was not assessed in prior studies of Mn and/or welding-related toxicity. Together, the current finding suggests that FA may capture early microstructural changes related to environmental toxicants before any changes in MD are discernible.

Lower GP FA Values in Welders Were Associated With Manganese Exposure

In welders, we report non-linear associations of GP FA values with both blood Mn levels and the PI, but no association with blood Fe or Cu levels, or with R2* values. Although we cannot rule out the influence of other unmeasured co-exposures, these findings suggest that, in welders, FA variations in the GP may be associated with exposure to Mn. This is consistent with previous findings reporting the GP as a primary region where welding-related Mn accumulates (Kim *et al.*, 1999; Lucchini *et al.*, 2000) and the region having microstructural changes in subjects with Mn toxicity (Criswell *et al.*, 2012; McKinney *et al.*, 2004; Stepens *et al.*, 2010). Negative correlations between FA values and the PI were reported previously for full-time welders (Kim *et al.*, 2011). In that study, however, FA values were examined only in white matter structures, not in the GP. To our knowledge, this is the first study to demonstrate associations between GP FA values and Mn-exposure measurements in welders.

It is worth noting that this study utilized PI and R1 measures for Mn, and R2* for Fe, accumulation in the BG but found no significant group differences in the GP compared with controls for these MRI measures. This is different from the majority of the welding-related literature where higher PI or R1 values in the GP were reported (Choi *et al.*, 2007; Criswell *et al.*, 2012), probably because our welders had relatively low-level exposure (Lee *et al.*, 2015). The lack of group differences in R1 and PI measures suggests that the GP FA group difference may not be due to current Mn brain accumulation per se since both R1 and PI signals decay with time (Han *et al.*, 2008; Kim, 2004; Nelson *et al.*, 1993) and so these MRI markers may not be able to sensitively reflect long-term cumulative effects of Mn exposure. Moreover, although GP FA values in welders declined after a critical level of blood Mn was reached and welders had higher blood Mn levels than controls, the blood Mn level, which may reflect short-term rather than long-term Mn-exposure (Mahoney and Small, 1968; Smith *et al.*, 2007), was not a significant predictor of GP FA values. Together, these results suggest that the observed GP FA group difference may not be due to short-term Mn-exposure effect, especially when the exposure level was low. Nevertheless, the current finding of GP FA-Mn-exposure measurements (blood Mn and PI) associations in welders suggests that the GP FA group difference may be exacerbated when the Mn exposure level is high.

It is intriguing to note that R1 values showed a similar non-linear relationship with GP FA, but the association was much weaker than that of the PI with GP FA. It is not clear which time-window of Mn-exposure the PI or R1 values mainly reflect. It is, however, possible that T1W intensity measures such as the PI may reflect a more lingering Mn effect, especially when the exposure level is high, whereas R1 may capture short-term dynamics more sensitively. Previous studies reported that T1W intensity values typically returned to baseline levels ca. 6 months after cessation of Mn exposure (Kim, 2004; Nelson *et al.*, 1993). Conversely, higher T1W intensity values in the BG

persisted in deceased miners who had a relatively prolonged time interval (median = 2.52 years ranging from 0 to 18.11 years) between last Mn exposure and death (Criswell *et al.*, 2015), although their Mn tissue concentrations at the time of autopsy were comparable to controls. Persistently higher T1W intensity values 2 years post-transplant also were found in some subjects with Mn toxicity secondary to liver failure (Maffeo *et al.*, 2014). It also was reported that T1W intensity indices reflected certain histopathological changes (Kim *et al.*, 1999). Conversely, the GP T1 relaxation time (1/R1) in Mn-exposed monkeys was lowest after 120 days of Mn-exposure, but returned to control values 2 months after cessation of Mn-exposure, suggesting that R1 may sensitively capture temporal dynamics of Mn brain accumulation and clearance (Han *et al.*, 2008). Consistent with this analysis, R1 also was associated more with short-term, rather than long-term, exposure metrics in our recent study (Lee *et al.*, 2015).

Lower FA Values Were Associated With Long-Term Welding Exposure

The present study demonstrated that, in welders, GP FA values started to decrease after a critical duration of YrsW was reached but they had no associations with the short-term exposure metrics. These results suggest that GP microstructural changes may be associated with long-, rather than short-, term exposure. Interestingly, ELT, another long-term exposure metric that estimates lifetime cumulative exposure, showed a similar relationship with GP FA values, although the association was not significant. Unlike YrsW, which did not consider welding-related intensity information, ELT estimation considered information related to exposure intensity such as welding type, base metal, use of personal protective equipment, and confined work space, which should theoretically estimate exposure better than YrsW. The risk of exposure misclassification, however, could increase in the ELT estimation since more parameters were included in calculating ELT than YrsW, which may have been the case in the current study particularly because it was not feasible to measure the airborne metal levels including Mn in the work place, an important factor to estimate ELT. Further studies with better exposure metrics (eg, on-site airborne metal measures) are needed to determine the exact dose-response associations.

In addition, the current results demonstrated that welders had significantly higher YrsW than controls, which was a significant predictor to explain GP FA values. Along with the nonlinear associations between GP FA and YrsW within welders, these results suggest that the GP FA group difference between welders and controls may be due, at least partly, to chronic welding exposure in welders. This finding is important because it implies that even very low levels of Mn-exposure may lead to microstructural changes if welding has the characteristic of chronic exposure (eg, YrsW > 30 years).

SUMMARY

This study demonstrated lower FA values in the GP of asymptomatic welders with chronic low-level exposure, and the association of these changes with long-term Mn exposure. These results suggest that FA may serve as a useful early marker to capture microstructural changes associated with chronic, subclinical Mn exposure in asymptomatic welders. Further studies are needed to replicate these findings and examine the neurobehavioral relevance of FA changes.

SUPPLEMENTARY DATA

Supplementary data are available online at http://toxsci.oxfordjournals.org/.

FUNDING

This work was supported by R01 ES019672 from the National Institute of Environmental Health Sciences and NS082151 from the National Institute of Neurological Disease and Stroke, the Hershey Medical Center General Clinical Research Center (National Center for Research Resources, Grant UL1 RR033184 that is now at the National Center for Advancing Translational Sciences, Grant UL1 TR000127), and the PA Department of Health Tobacco CURE Funds.

ACKNOWLEDGMENTS

We would like to thank all of the volunteers who participated in this study. In addition, we are indebted to many individuals who helped make this study possible, including: Melissa Santos and Susan Kocher for subject coordination, recruitment, blood sample handling, and data entry; Pam Susi and Pete Stafford of CPWR; Mark Garrett, John Clark, and Joe Jacoby of the International Brotherhood of Boilermakers; Fred Cosenza and all members of the Safety Committee for the Philadelphia Building and Construction Trades Council; Ed McGehean of the Steamfitters Local Union 420; Jim Stewart of the Operating Engineers; Sean Gerie of the Brotherhood of Maintenance of Way Employees Division Teamsters Rail Conference; and Terry Peck of Local 520 Plumbers, Pipefitters and HVAC.

REFERENCES

Backens, M. (2015). [Basic principles and technique of diffusion-weighted imaging and diffusion tensor imaging]. *Der Radiol.* **55**, 762–770.

Basser, P. J. (1995). Inferring microstructural features and the physiological state of tissues from diffusion-weighted images. *NMR Biomed.* **8**, 333–344.

Basser, P. J., and Pierpaoli, C. (1996). Microstructural and physiological features of tissues elucidated by quantitative-diffusion-tensor MRI. *J. Magn. Reson. B* **111**, 209–219.

Cersosimo, M. G., and Koller, W. C. (2006). The diagnosis of manganese-induced parkinsonism. *Neurotoxicology* **27**, 340–346.

Chan, L. L., Rumpel, H., Yap, K., Lee, E., Loo, H. V., Ho, G. L., Fook-Chong, S., Yuen, Y., and Tan, E. K. (2007). Case control study of diffusion tensor imaging in Parkinson's disease. *Journal of Neurology, Neurosurgery & Psychiatry* **78**, 1383–1386.

Chang, Y., Kim, Y., Woo, S. T., Song, H. J., Kim, S. H., Lee, H., Kwon, Y. J., Ahn, J. H., Park, S. J., Chung, I. S., *et al.* (2009). High signal intensity on magnetic resonance imaging is a better predictor of neurobehavioral performances than blood manganese in asymptomatic welders. *Neurotoxicology* **30**, 555–563.

Choi, D. S., Kim, E. A., Cheong, H. K., Khang, H. S., Ryoo, J. W., Cho, J. M., Sakong, J., and Park, I. (2007). Evaluation of MR signal index for the assessment of occupational manganese exposure of welders by measurement of local proton T 1 relaxation time. *Neurotoxicology* **28**, 284–289.

Criswell, S. R., Nelson, G., Gonzalez-Cuyar, L. F., Huang, J., Shimony, J. S., Checkoway, H., Simpson, C. D., Dills, R., Seixas, N. S., and Racette, B. A. (2015). Ex vivo magnetic

resonance imaging in South African manganese mine workers. *Neurotoxicology* **49**, 8–14.

Criswell, S. R., Perlmutter, J. S., Huang, J. L., Golchin, N., Flores, H. P., Hobson, A., Aschner, M., Erikson, K. M., Checkoway, H., and Racette, B. A. (2012). Basal ganglia intensity indices and diffusion weighted imaging in manganese-exposed welders. *Occup. Environ. Med.* **69**, 437–443.

Dorman, D. C., Struve, M. F., Wong, B. A., Dye, J. A., and Robertson, I. D. (2006). Correlation of brain magnetic resonance imaging changes with pallidal manganese concentrations in rhesus monkeys following subchronic manganese inhalation. *Toxicol. Sci.* **92**, 219–227.

Du, G., Lewis, M. M., Styner, M., Shaffer, M. L., Sen, S., Yang, Q. X., and Huang, X. (2011). Combined R2* and diffusion tensor imaging changes in the substantia nigra in Parkinson's disease. *Mov. Disord.* **26**, 1627–1632.

Flynn, M. R., and Susi, P. (2009). Manganese, iron, and total particulate exposures to welders. *J. Occup. Environ. Hyg.* **7**, 115–126.

Ge, Y., Udupa, J. K., Nyul, L. G., Wei, L., and Grossman, R. I. (2000). Numerical tissue characterization in MS via standardization of the MR image intensity scale. *J. Magn. Reson. Imaging* **12**, 715–721.

Gouttard, S., Styner, M., Joshi, S., Smith, R.G., Hazlett, H.C., Gerig, G. (2007) Subcortical structure segmentation using probabilistic atlas priors. Medical Imaging. *International Society for Optics and Photonics*, pp. 65122J-65122J-65111.

Haacke, E. M., Cheng, N. Y., House, M. J., Liu, Q., Neelavalli, J., Ogg, R. J., Khan, A., Ayaz, M., Kirsch, W., and Obenaus, A. (2005). Imaging iron stores in the brain using magnetic resonance imaging. *Magn. Reson. Imaging* **23**, 1–25.

Han, J. H., Chung, Y. H., Park, J. D., Kim, C. Y., Yang, S. O., Khang, H. S., Cheong, H. K., Lee, J. S., Ha, C. S., Song, C. W., *et al.* (2008). Recovery from welding-fume-exposure-induced MRI T1 signal intensities after cessation of welding-fume exposure in brains of cynomolgus monkeys. *Inhal. Toxicol.* **20**, 1075–1083.

Hashimoto, R., Mori, T., Nemoto, K., Moriguchi, Y., Noguchi, H., Nakabayashi, T., Hori, H., Harada, S., Kunugi, H., and Saitoh, O. (2009). Abnormal microstructures of the basal ganglia in schizophrenia revealed by diffusion tensor imaging. *World J. Biol. Psychiatry* **10**, 65–69.

Holm, S. (1979). A simple sequentially rejective multiple test procedure. *Scand. J. Stat.* 65–70.

Joshi, S., Davis, B., Jomier, M., and Gerig, G. (2004). Unbiased diffeomorphic atlas construction for computational anatomy. *Neuroimage* **23(Suppl 1)**, S151–S160.

Kim, S. H., Chang, K. H., Chi, J. G., Cheong, H. K., Kim, J. Y., Kim, Y. M., and Han, M. H. (1999). Sequential change of MR signal intensity of the brain after manganese administration in rabbits: Correlation with manganese concentration and histopathologic findings. *Invest. Radiol.* **34**, 383.

Kim, Y. (2004). High signal intensities on T1-weighted MRI as a biomarker of exposure to manganese. *Indus. Health* **42**, 111–115.

Kim, Y., Jeong, K. S., Song, H. J., Lee, J. J., Seo, J. H., Kim, G. C., Lee, H. J., Kim, H. J., Ahn, J. H., and Park, S. J. (2011). Altered white matter microstructural integrity revealed by voxel-wise analysis of diffusion tensor imaging in welders with manganese exposure. *Neurotoxicology* **32**, 100–109.

Krieger, D., Krieger, S., Theilmann, L., Jansen, O., Gass, P., and Lichtnecker, H. (1995). Manganese and chronic hepatic encephalopathy. *Lancet* **346**, 270–274.

Le Bihan, D., Mangin, J. F., Poupon, C., Clark, C. A., Pappata, S., Molko, N., and Chabriat, H. (2001). Diffusion tensor imaging: Concepts and applications. *J. Magn. Reson. Imaging* **13**, 534–546.

Lee, E. Y., Flynn, M. R., Du, G., Li, Y., Lewis, M. M., Herring, A. H., Van Buren, E., Van Buren, S., Kong, L., and Fry, R. C. (2016). Increased R2* in the caudate nucleus of asymptomatic welders. *Toxicol. Sci.* **150**(2), 369–377.

Lee, E. Y., Flynn, M. R., Du, G., Lewis, M. M., Fry, R., Herring, A. H., Van Buren, E., Van Buren, S., Smeester, L., Kong, L., *et al.* (2015). T1 Relaxation Rate (R1) Indicates nonlinear Mn accumulation in brain tissue of welders with low-level exposure. *Toxicol. Sci.* **146**, 281–289.

Liu, Z., Wang, Y., Gerig, G., Gouttard, S., Tao, R., Fletcher, T., and Styner, M. (2010). Quality control of diffusion weighted images. *Proc SPIE Int Soc Opt Eng* **7628**,

Lucchini, R., Albini, E., Placidi, D., Gasparotti, R., Pigozzi, M. G., Montani, G., and Alessio, L. (2000). Brain magnetic resonance imaging and manganese exposure. *Neurotoxicology* **21**, 769–775.

Lucchini, R. G., Martin, C. J., and Doney, B. C. (2009). From manganism to manganese-induced parkinsonism: A conceptual model based on the evolution of exposure. *Neuromol. Med.* **11**, 311–321.

Maffeo, E., Montuschi, A., Stura, G., and Giordana, M. T. (2014). Chronic acquired hepatocerebral degeneration, pallidal T1 MRI hyperintensity and manganese in a series of cirrhotic patients. *Neurol. Sci.* **35**, 523–530.

Mahoney, J. P., and Small, W. J. (1968). Studies on manganese. 3. The biological half-life of radiomanganese in man and factors which affect this half-life. *J. Clin. Invest.* **47**, 643–653.

McKinney, A. M., Filice, R. W., Teksam, M., Casey, S., Truwit, C., Clark, H. B., Woon, C., and Liu, H. Y. (2004). Diffusion abnormalities of the globi pallidi in manganese neurotoxicity. *Neuroradiology* **46**, 291–295.

Nelson, K., Golnick, J., Korn, T., and Angle, C. (1993). Manganese encephalopathy: Utility of early magnetic resonance imaging. British journal of industrial. *Medicine* **50**, 510–513.

Nyúl, L. G., Udupa, J. K., and Zhang, X. (2000). New variants of a method of MRI scale standardization. *Med. Imaging IEEE Trans.* **19**, 143–150.

Racette, B. A., Criswell, S. R., Lundin, J. I., Hobson, A., Seixas, N., Kotzbauer, P. T., Evanoff, B. A., Perlmutter, J. S., Zhang, J., Sheppard, L., *et al.* (2012). Increased risk of parkinsonism associated with welding exposure. *Neurotoxicology* **33**, 1356–1361.

Rueckert, D., Sonoda, L. I., Hayes, C., Hill, D. L., Leach, M. O., and Hawkes, D. J. (1999). Nonrigid registration using free-form deformations: Application to breast MR images. *Med. Imaging IEEE Trans.* **18**, 712–721.

Salvador, R., Pena, A., Menon, D. K., Carpenter, T. A., Pickard, J. D., and Bullmore, E. T. (2005). Formal characterization and extension of the linearized diffusion tensor model. *Hum. Brain Mapp.* **24**, 144–155.

Schaefer, P. W., Grant, P. E., and Gonzalez, R. G. (2000). Diffusion-weighted MR imaging of the brain. *Radiology* **217**, 331–345.

Schwyn, R. C., and Fox, C. A. (1974). The primate substantia nigra: A Golgi and electron microscopic study. *J. Hirnforsch.* **15**, 95–126.

Sen, S., Flynn, M. R., Du, G., Tröster, A. I., An, H., and Huang, X. (2011). Manganese accumulation in the olfactory bulbs and other brain regions of "asymptomatic" welders. *Toxicol. Sci.* **121**, 160–167.

Smith, D., Gwiazda, R., Bowler, R., Roels, H., Park, R., Taicher, C., and Lucchini, R. (2007). Biomarkers of Mn exposure in humans. *Am. J. Indus. Med.* **50**, 801–811.

Stejskal, E. O., and Tanner, J. E. (1965). Spin diffusion measurements: Spin echoes in the presence of a time-dependent field gradient. *J. Chem. Phys.* **42**, 288–292.

Stepens, A., Stagg, C. J., Platkājis, A., Boudrias, M. H., Johansen-Berg, H., and Donaghy, M. (2010). White matter abnormalities in methcathinone abusers with an extrapyramidal syndrome. *Brain* **133**, 3676–3684.

Vaillancourt, D. E., Spraker, M. B., Prodoehl, J., Abraham, I., Corcos, D. M., Zhou, X. J., Comella, C. L., and Little, D. M. (2009). High-resolution diffusion tensor imaging in the substantia nigra of de novo Parkinson disease. *Neurology* **72**, 1378–1384.

Venkatesan, R., Lin, W., and Haacke, E. M. (1998). Accurate determination of spin-density and T1 in the presence of RF-field inhomogeneities and flip-angle miscalibration. *Magn. Reson. Med.* **40**, 592–602.

Wang, J. D., Huang, C. C., Hwang, Y., Chiang, J. R., Lin, J. M., and Chen, J. (1989). Manganese induced parkinsonism: An outbreak due to an unrepaired ventilation control system in a ferromanganese smelter. *Br. J. Indus. Med.* **46**, 856–859.

Yelnik, J., Percheron, G., and Francois, C. (1984). A Golgi analysis of the primate globus pallidus. II. Quantitative morphology and spatial orientation of dendritic arborizations. *J. Comp. Neurol.* **227**, 200–213.

Yoshikawa, K., Nakata, Y., Yamada, K., and Nakagawa, M. (2004). Early pathological changes in the parkinsonian brain demonstrated by diffusion tensor MRI. *J. Neurol. Neurosurg. Psychiatry* **75**, 481–484.